communications biology

ARTICLE

https://doi.org/10.1038/s42003-021-01985-7 OPEN

Global climate and nutrient controls of photosynthetic capacity

Yunke Peng[1,2,3], Keith J. Bloomfield[4], Lucas A. Cernusak[5], Tomas F. Domingues[6] & I. Colin Prentice[4,7,8]✉

There is huge uncertainty about how global exchanges of carbon between the atmosphere and land will respond to continuing environmental change. A better representation of photosynthetic capacity is required for Earth System models to simulate carbon assimilation reliably. Here we use a global leaf-trait dataset to test whether photosynthetic capacity is quantitatively predictable from climate, based on optimality principles; and to explore how this prediction is modified by soil properties, including indices of nitrogen and phosphorus availability, measured in situ. The maximum rate of carboxylation standardized to 25 °C (V_{cmax25}) was found to be proportional to growing-season irradiance, and to increase—as predicted—towards both colder and drier climates. Individual species' departures from predicted V_{cmax25} covaried with area-based leaf nitrogen (N_{area}) but community-mean V_{cmax25} was unrelated to N_{area}, which in turn was unrelated to the soil C:N ratio. In contrast, leaves with low area-based phosphorus (P_{area}) had low V_{cmax25} (both between and within communities), and P_{area} increased with total soil P. These findings do not support the assumption, adopted in some ecosystem and Earth System models, that leaf-level photosynthetic capacity depends on soil N supply. They do, however, support a previously-noted relationship between photosynthesis and soil P supply.

[1] Masters Programme in Ecosystems and Environmental Change, Department of Life Sciences, Imperial College London, Ascot, UK. [2] Department of Environmental Systems Science, ETH, Zurich, Switzerland. [3] Swiss Federal Institute for Forest, Snow and Landscape Research (WSL), Birmensdorf, Switzerland. [4] Department of Life Sciences, Imperial College London, Ascot, UK. [5] Centre for Tropical Environmental Sustainability Studies, James Cook University, Cairns, QLD, Australia. [6] FFCLRP, Department of Biology, University of São Paulo, Ribeirão Preto, Brazil. [7] Department of Biological Sciences, Macquarie University, North Ryde, NSW, Australia. [8] Department of Earth System Science, Tsinghua University, Beijing, China. ✉email: c.prentice@imperial.ac.uk

Accurate representation of photosynthetic capacity is critical for modelling the response of terrestrial ecosystems to environmental change[1,2]. Earth System models use the FvCB biochemical model[3] to simulate responses of C_3 photosynthesis to environment. The modelled instantaneous carbon-assimilation rate is limited either by V_{cmax} (μmol m^{-2} s^{-1}), the maximum rate of carboxylation, or J, the light-dependent electron transport rate, which is asymptotic at high light towards J_{max} (μmol m^{-2} s^{-1}). Both assimilation rates depend on temperature and on the intercellular partial pressure of CO_2 (C_i).

Application of the FvCB model[3] requires knowledge of three 'plant-determined' quantities: V_{cmax}, J_{max} and the ratio of C_i to the ambient partial pressure of CO_2 (C_a). This ratio, here called χ, is regulated by stomata. J_{max} and V_{cmax} are closely coordinated[4,5]. More data are available on V_{cmax} because it can be inferred from the light-saturated photosynthetic rate, which is commonly measured in the field[6]. Global models have to contend with the large observed variation (in time and space, and within and between species) of V_{cmax}. Data analyses have explored its relationship to leaf nutrients[7–9] and environmental variables[10,11]. Until recently, however, most models have assigned constant values of V_{cmax} at standard temperature (conventionally 25 °C: thus V_{cmax25}) for each of a small number of plant functional types (PFTs), and allowed the temperature-dependent values to follow standard (instantaneous) equations of enzyme kinetics. Models also have to represent the plant-type and environmental dependencies of χ (ref. [12]). Most models assign constant per-PFT values of parameters in one of the two widely used models for the response of stomatal conductance to vapour pressure deficit (D). However, these simplifications are not the best possible. V_{cmax25} and χ commonly vary at least as much within as between PFTs; while χ has predicted (and observed) relationships to growth temperature (T_g) and to elevation above sea level (z) through its effect on atmospheric pressure, which are neglected in the standard models[10].

One strand of recent research has accordingly focused on a search for universal responses to environment, applicable to all (C_3) plants. Eco-evolutionary optimality hypotheses[12–15] have been invoked in recent efforts to derive general principles for the prediction of plant traits and productivity[10,11,16–18]. The least-cost hypothesis[12,19] proposes that investments in transpiration capacity (maintaining the water transport pathway) and V_{cmax} are balanced so that photosynthesis is achieved at the lowest total cost in maintenance respiration of leaves and stems. Within this framework, χ varies over a limited range, consistent with tight regulation of the balance between water loss and carbon gain[12]. The hypothesis predicts that χ should decline with increasing D, decreasing T_g and increasing z. Each of these predictions is quantitatively supported by global compilations of χ values inferred from stable carbon isotope measurements in leaves[10,20,21] and wood[22]. The coordination hypothesis provides a framework to predict V_{cmax} from physical environmental variables: irradiance (photosynthetic photon flux density, PPFD) and temperature and CO_2 (ref. [23]). The 'strong form'[24] of this hypothesis states that carboxylation and electron transport are co-limiting under typical daytime growth conditions, so that neither is in excess. V_{cmax25} is observed to increase with PPFD, D and z (refs. [10,11,21]), and to decline with T_g (refs. [24,25]). The coordination hypothesis predicts all these observations. The decline with T_g is predicted because less Rubisco (the key carboxylation enzyme) is required to support photosynthesis in warmer environments[24]. The increases with D and z are predicted because greater photosynthetic capacity is required to support a given rate of carbon assimilation at lower χ (ref. [26]).

Positive relationships between photosynthetic capacities and leaf N (N_{area})[27,28] and leaf P (P_{area})[29–32] are also widely observed. Much leaf N is invested in Rubisco[33–36]. Leaf P is required inter alia for cell membranes, nucleic acid synthesis and for ATP and NADPH production[9,37]. The predictive power of relationships to N_{area} or P_{area} is often weak[11,38–40]; however, recent studies[8,9] have proposed a framework in which V_{cmax25} is constrained by the lesser of two functions, one related to N_{area} and the other to P_{area}. Leaf nutrient levels, in turn, may or may not reflect their availability in the soil. N_{area} can be related to soil pH (or fertility) but is not unambiguously related to soil N availability[14], while P_{area} is related to both soil fertility and total soil P[14,41].

Thus, there are two conflicting paradigms to explain worldwide variation in photosynthetic capacity. One emphasizes its predictability from climate, based on optimality principles. The other emphasizes its predictability from leaf nutrients. This second approach has been extended to embrace the assumption that leaf nutrients reflect soil nutrient availability—although this is not universally true[42].

To help resolve this contradiction, we assembled a large global dataset of V_{cmax25}, N_{area} and P_{area} data from multiple species and sites. In situ soil measurements (pH, C:N ratio and total P) were available at a subset of the sites. Rather than total soil N, which mainly relates to soil organic content, we used soil C:N as an inverse measure of N availability[43]. We hypothesized that

(1) Photosynthetic capacity is subject to first-order control by climate, as predicted by the coordination and least-cost hypotheses. V_{cmax25} increases in proportion to PPFD and increases towards colder and drier environments, due to greater biochemical investment required when χ is low.
(2) Photosynthetic capacity is reduced, compared to climate-based predictions, under conditions of low nutrient (N and/or P) availability.

Results

Theoretically predicted values (see 'Methods') of the derivatives of ln V_{cmax25} against ln PPFD, T_g and ln D are given in Table 1, for comparison with values fitted by statistical models (Table 1, Fig. 1). The value of 1 for the derivative of ln V_{cmax25} with respect to ln PPFD implies proportionality, i.e. a 10% increase in PPFD induces a 10% increase in V_{cmax25}. The value of –0.05 K^{-1} for the derivative of ln V_{cmax25} with respect to T_g implies that a 1 °C

Table 1 Summary statistics for the climatic dependencies of V_{cmax25} (μmol m^{-2} s^{-1}).

Predictor for V_{cmax25}	Theoretical value	All-species coefficient $R^2 = 0.17$	Site-mean coefficient $R^2 = 0.31$
ln PPFD	1	0.99 ± 0.22	1.02 ± 0.21
T_g	-0.05 K^{-1}	-0.04 ± 0.01 K^{-1}	-0.04 ± 0.01 K^{-1}
ln D	0.07	0.13 ± 0.06	0.13 ± 0.06

Log-transformed photosynthetic capacities standardized to 25 °C were derived for all species and as site means. Theoretical values were obtained by evaluating partial derivatives of Eq. (3) with respect to each variable at the median climate of the global dataset (PPFD = 400 μmol m^{-2} s^{-1}, T_g = 25 °C, D = 0.60 kPa). All-species coefficients represent the partial effects of each variable, estimated in a mixed effects model with site and species as random effects. Site-mean coefficients represent the partial effect of each variable, estimated in a fixed effects model. All fitted values are given ±1 standard error.

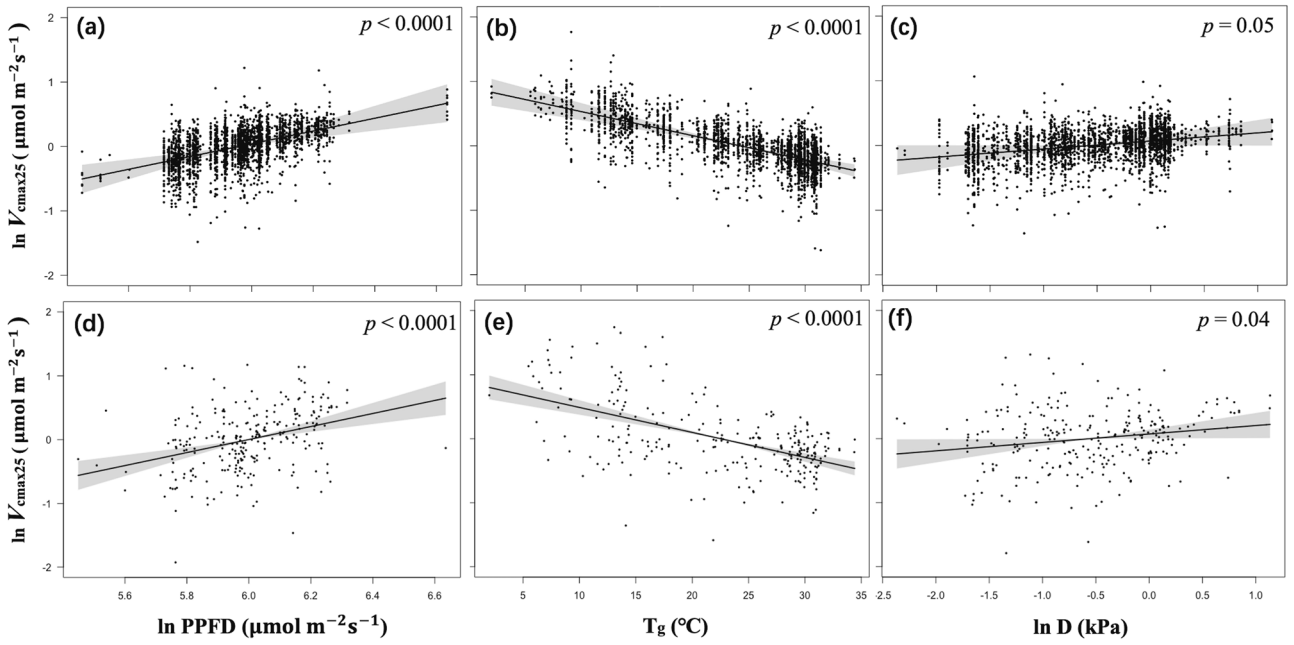

Fig. 1 Partial residual plots for V_{cmax25} in relation to climate variables. Partial residual plots for log-transformed V_{cmax25}: all-species (**a**, **b**, **c**) and site-means (**d**, **e**, **f**). Coefficients and standard errors for the fitted lines are given in Supporting Information Table S4.

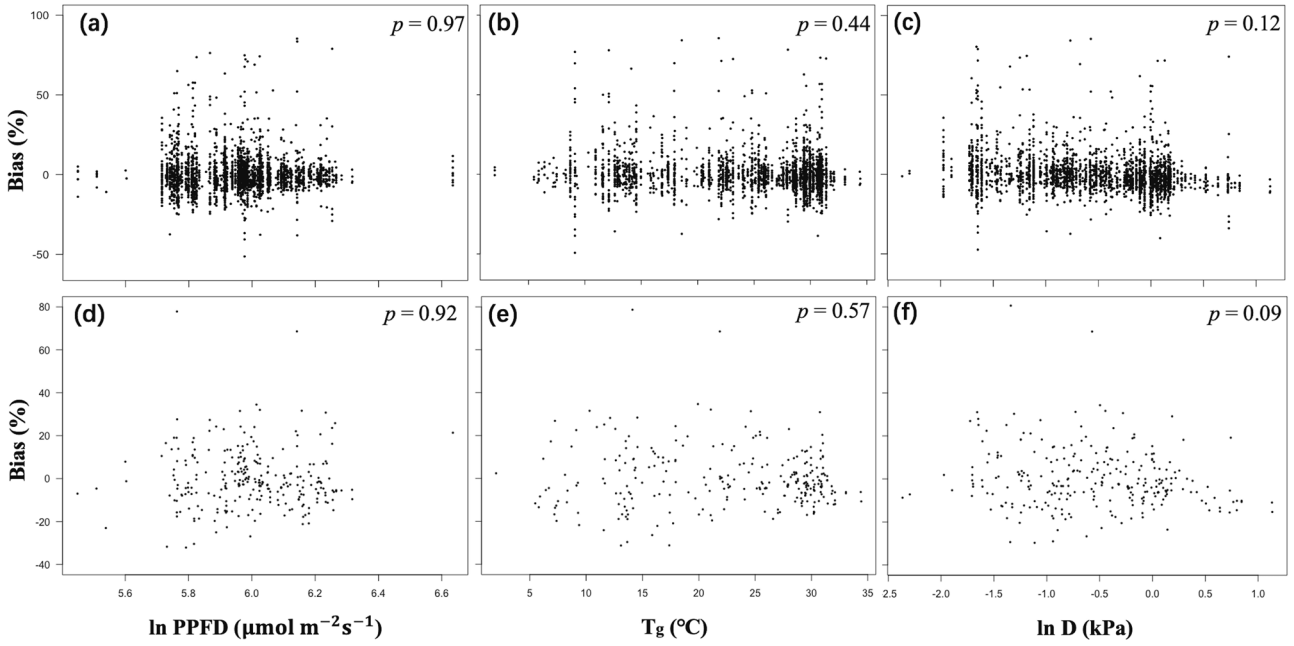

Fig. 2 Partial residual plots for the model bias of theoretically predicted V_{cmax25} values in relation to climate variables. Partial residual plots for the model bias of theoretically predicted V_{cmax25} values in relation to climate variables: all-species (**a**, **b**, **c**) and site means (d, e, f). Coefficients and standard errors for the fitted lines are given in Supporting Information Table S4.

increase in growth temperature is predicted to induce a 5% decrease in V_{cmax25}. Regression coefficients of V_{cmax25} against the same climate variables were statistically indistinguishable from theoretically predicted values (Table 1). Analysis of site-mean data explained more variance than a mixed-model analysis of all species (see 'Methods'), indicating that a greater fraction of variation in photosynthetic capacity can be explained by physical environmental constraints when considering the whole community together, excluding variation within the community. The response of V_{cmax25} to D was slightly steeper in the 'observed' than the 'theoretical' relationship, but the difference was within one standard error. From the random term of the all-species mixed model (see 'Methods'), species and site identity separately accounted for 22 and 50% of the variation in V_{cmax25} that was unexplained by the model's climate variables (Table S1).

No significant bias was shown for the predicted relationship of V_{cmax25} to PPFD, T_g or D (Fig. 2). There was a possible underestimation of V_{cmax25} at higher D, but this trend was not significant either in all-species (Fig. 2c; $p = 0.12$) or site-mean (Fig. 2f; $p = 0.09$) analyses.

Statistical models of photosynthetic capacity (all species and site means) as a function of climate overestimated V_{cmax25} in low-

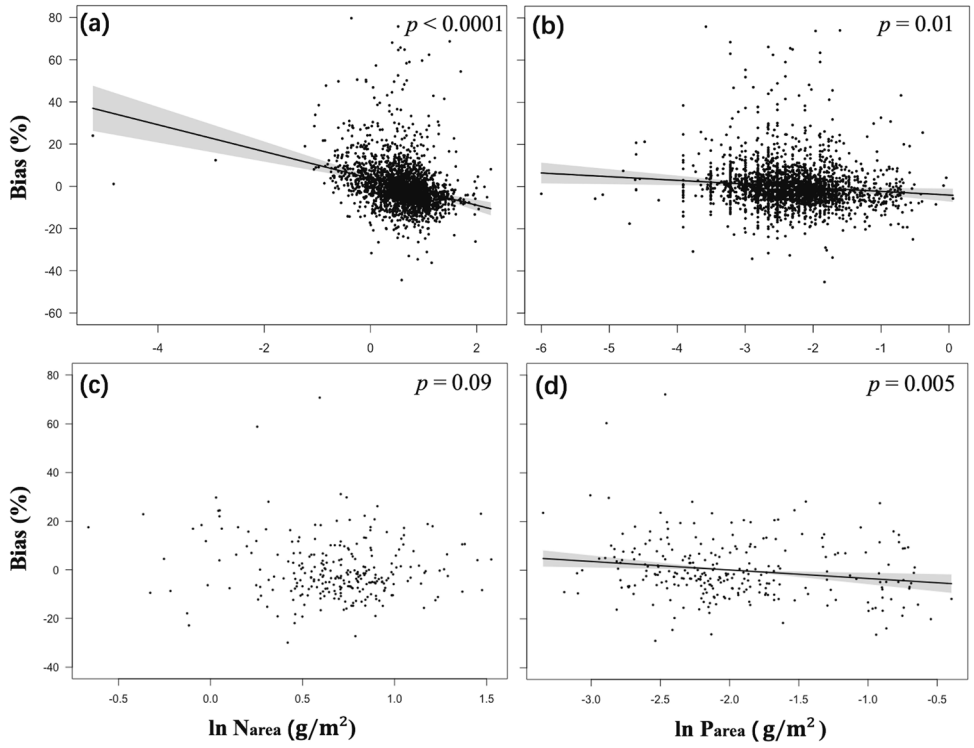

Fig. 3 Partial residual plots for the model bias of statistically fitted V_{cmax25} in relation to leaf nutrients. Partial residual plots for the model bias of statistically fitted V_{cmax25} (Table 1) in relation to leaf nutrients, for all-species (**a**, **b**) and site-mean (**c**, **d**) data. The model bias represents the difference between predicted and observed V_{cmax25}, where the predicted V_{cmax25} was based on the climate-driven regressions fitted from site-mean and all-species data as shown in Table 1. Coefficients and standard errors for the fitted lines are given in Supporting Information Table S4.

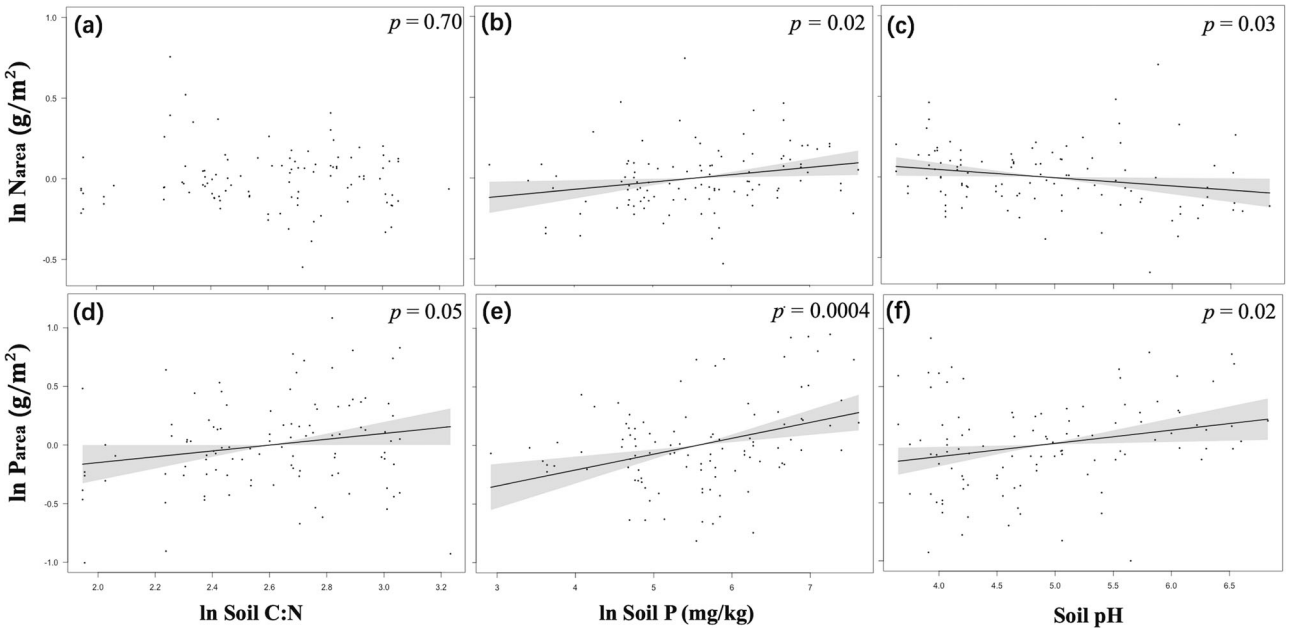

Fig. 4 Partial residual plots for leaf nutrients in relation to in situ measured soil properties. Partial residual plots for leaf nutrients (site means) in relation to in situ measured soil properties, for Narea (**a**, **b**, **c**) and Parea (**d**, **e**, **f**) data. Analyses for all species are shown in Fig. S1. Coefficients and standard errors for the fitted lines are given in Supporting Information Table S4.

P leaves and underestimated V_{cmax25} in high-P leaves (Fig. 3b, d). The all-species statistical model also showed a bias in V_{cmax25} related to leaf N (Fig. 3a). This relationship was still apparent ($p <$ 0.0001) after removal of three highly influential points. The three species with extremely low N_{area} values (*Turpinia pomifera, Uncaria laevigata* and *Walsura pinnata*) shown in Fig. 3a were sampled in Yunnan, China (21.6°N, 101.5°E). These species possessed very low V_{cmax25} (21 μmol m^{-2} s^{-1}) values, probably a

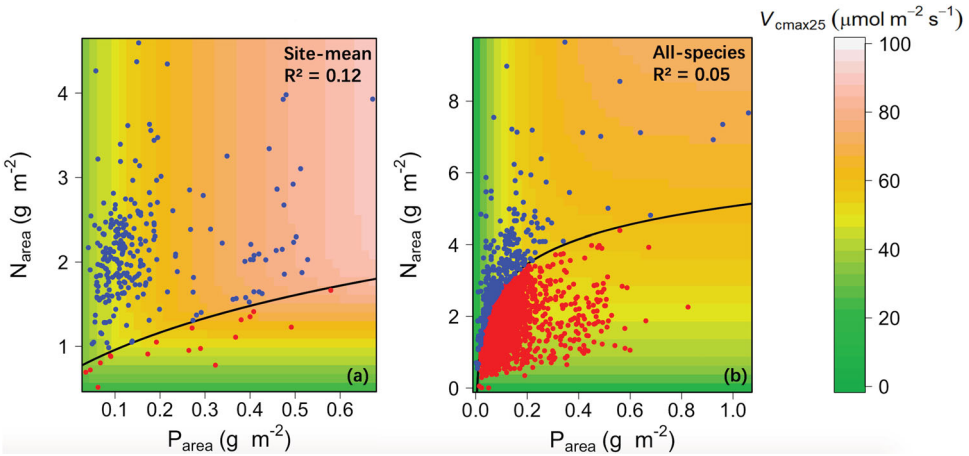

Fig. 5 Visualizing the co-limitation of V_{cmax25} by Narea and Parea based on the minimum function model. Visualizing the co-limitation of V_{cmax25} by Narea and Parea for global (**a**) site-mean and (**b**) all-species analyses, based on the minimum function model. Following Domingues et al.8, blue points represent cases where Parea was the 'limiting' nutrient; red points represent cases where Narea was the 'limiting' nutrient. The fitted regression line in (**a**) is Narea = ln (5.96 Parea + 2.01) and in (**b**) is Narea = ln (158.62 Parea + 0.11).

consequence of growth in deep shade. In contrast to the all-species model, the site-mean model showed no bias with respect to N_{area} (Fig. 3c).

Analysis of the subset of the data with in situ soil measurements indicated that P_{area} increased with soil C:N ratio, total soil P and soil pH (Figs. 4d–f, S1d–f). N_{area} increased with soil P (Figs. 4b, S1b) and decreased with soil pH (Figs. 4c, S1c). No relationship was found between leaf N and soil C:N ratio (Figs. 4a, S1a).

Global V_{cmax25} could, alternatively, be represented by a minimum function (Eq. 12) of N_{area} and P_{area}. This function provided a better fit to the data than linear regression models with V_{cmax25} as a function of N_{area} and P_{area} and combinations thereof or a model including N_{area}, P_{area} and their interaction (Table S2). In site-mean analysis based on the minimum function P_{area} was shown to be the principal limiting factor (93% of sites). In all-species analysis, N_{area} was shown to be the principal limiting factor (86% of species; Fig. 5). This contrast agrees with our findings for model bias: V_{cmax25} variations within sites are more related to leaf N, while variations between sites (community means) are related to mean leaf P but not to mean leaf N. However, the goodness of fit of these models based on nutrients alone ($R^2 = 0.05$, 0.12 for all species and site mean, respectively) was inferior to that of models based on climate alone ($R^2 = 0.17$, 0.31).

Discussion

The optimality framework accounts for the major global patterns of photosynthetic capacity as shown in our dataset. Consistent with hypothesis (1), global patterns of V_{cmax25} were found to be predictable to first order from PPFD, growth temperature and vapour pressure deficit. Proportionality to PPFD is consistent with observations on light gradients[44], seasonal dynamics[45] and the cloud immersion effect, which decreases PPFD and V_{cmax25} at mid elevations of tropical mountains[39]. V_{cmax25} was predicted (and found) to be greater in drier environments: consistent with the larger biochemical investment required to achieve optimal photosynthesis when stomata are more closed. We found a somewhat steeper than predicted response to D and thus a slight but non-significant underestimation of V_{cmax25} at higher D. This might be because the least-cost hypothesis does not consider the compounding effect of low soil moisture, which often accompanies high D and further decreases stomatal conductance, therefore preventing excessive transpiration but increasing the investment in carboxylation capacity[22,46,47]. In short-term drying experiments, V_{cmax25} typically declines steeply (at different critical pre-dawn water potential values dependent on species[48,49]), although an increase in leaf-level V_{cmax25}—which may be accompanied by a reduction in leaf area—can be observed when plants are allowed to acclimate to moderate drought[50–55]. These findings are consistent with the expectation[56] that a decrease of V_{cmax} under drought conditions is linked to a declining hydraulic capacity of the soil–root–xylem system, which can be accommodated over time by leaf shedding. V_{cmax25} showed a negative response to growth temperature, which is predicted because greater investment in photosynthetic enzymes is required at lower temperatures to produce the same catalytic activity[10,55]. Thermal acclimation according to this optimality principle is supported by evidence for a decline of light use efficiency[57] and an increase of photosynthetic nitrogen use efficiency[58] towards warmer environments, and by increased V_{cmax25} at higher elevations[21,41]. The percentage variance explained by these relationships is modest, however (31% for site-mean data: Table 1), consistent with findings by van der Plas et al.[59] on the limits to predictability of ecosystem function from plant traits.

Our hypothesis (2) is partially supported by the analysis of bias in the statistically fitted model. Consistent with findings by Maire et al.[14], we showed an overestimation of V_{cmax25} in leaves with low P_{area}. These are typical of sites on acid soils and/or low soil P availability, including some wet tropical forests[14,39]. Many tropical soils are characterized by low total soil P due to long-term weathering[60,61], and a dependency of net primary production on P availability has been shown in tropical forests[62]. Small-scale experimental studies have also suggested that low soil P availability can decrease the light-saturated photosynthetic rate (A_{sat})[63–65] and V_{cmax}[66,67]. Adaptation strategies to cope with long-term P deficiency include restricting export of triose phosphate to the cytosol[68], preventing the phosphorylation of ADP to ATP[37,69], phosphate recycling during photorespiration[70] and the replacement of phospholipids by galactolipids and sulpholipids[71,72], all potentially entailing additional costs to the plant. On the other hand, photosynthesis in tropical forests is typically not limited by N[73].

The global relationship between V_{cmax25} and N_{area}[74] primarily reflects the large amount of N invested in Rubisco and other photosynthetic enzymes[75]. Leaves with a high photosynthetic capacity necessarily have a large N content per unit area. Within vegetation canopies, V_{cmax25} and N_{area} both vary greatly,

especially along the light gradient from the canopy top to the understory—as shown in many empirical studies[23,35,76,77] and further discussed elsewhere[78,79]. Our data provide no information on the range of light environments within sites and, therefore, our finding of a bias (low-N leaves having lower than predicted V_{cmax25}) in the all-species analysis is no surprise. However, the relationship disappeared in the site-mean analysis, indicating that V_{cmax25} at community level is predictable without the need to consider leaf N. Moreover, we found no support for the hypothesis (assumed in some ecosystem and Earth System models) that leaf N is determined by soil N availability—suggesting that the metabolic component of leaf N is determined by photosynthetic capacity, as proposed by Dong et al.[28], rather than vice versa. We did however find that leaf N increases with soil P, which is consistent with the observed effect of soil P on photosynthetic capacity.

A limitation of our analysis is its implicit assumption that mesophyll conductance (g_m) is not limiting to photosynthesis. V_{cmax} as estimated here, therefore, is an 'apparent' value and likely to underestimate the true photosynthetic capacity by a variable amount, which cannot be predicted from data currently available at a large scale. However, this simplification reflects the situation in the great majority of ecosystem models, and it has been indicated that 'greater process knowledge of g_m will be required before it can be included [in models]' (ref. [80], p. 26). A more comprehensive understanding of the relationships between leaf nutrients and photosynthesis will depend on advances in understanding the anatomical and physiological controls of g_m (refs. [81,82]), and extensions of leaf-level optimality theory to consider these controls.

In conclusion, while the short-term control of photosynthesis is relatively well understood (and modelled), the longer-term control of photosynthetic capacity is different, and subject to conflicting interpretations. Our findings show that the first-order climatic controls of V_{cmax25} are relatively strong and predictable, indicating that models must account for them. Our results are not consistent with the model assumption that soil N availability controls leaf N, which in turn controls V_{cmax25}. They are, however, consistent with previous observational and experimental results indicating the existence of P limitation on leaf P, leaf N and V_{cmax25}.

Methods

During photosynthesis, C_i declines relative to C_a because C assimilation removes CO_2 from the intercellular spaces while the stomata impose a resistance to the diffusion of CO_2 into the leaf from the air. The C_i/C_a ratio (χ) is maintained within a limited range (about 0.5–0.9 in C_3 plants) that is determined by the growth environment[83]. According to the least-cost hypothesis[12,19], χ is controlled by stomata in such a way as to minimize the sum of the unit costs of the required capacities for transpiration and carboxylation. A consequence of this hypothesis is that for any given set of environmental conditions, there is an optimal value of χ[10,12]

$$\chi_{opt} = \frac{\Gamma^*}{C_a} + \frac{(1 - \frac{\Gamma^*}{C_a})\xi}{\xi + \sqrt{D}}, \text{where } \xi = \sqrt{\left[\frac{\beta(K + \Gamma^*)}{1.6\,\eta^*}\right]} \quad (1)$$

that satisfies the least-cost criterion. Here, Γ* is the photorespiratory compensation point, i.e. the value of C_i at which gross photosynthesis is zero; K is the effective Michaelis–Menten coefficient of Rubisco (Pa); D is the leaf-to-air vapour pressure deficit (Pa); η* is the viscosity of water relative to its value at 25 °C and β is the ratio of the unit costs of maintaining carboxylation and transpiration activities at 25 °C, estimated as 146 based on a global compilation of leaf stable carbon isotope measurements[10]. K is given by

$$K = K_C(1 + O/K_O) \quad (2)$$

where K_C and K_O are the Michaelis–Menten coefficients of Rubisco for CO_2 and O_2, respectively (Pa, reflecting the twin affinities of Rubisco), and O is the partial pressure of O_2 (Pa). Γ*, K_C and K_O are functions of temperature, which we apply based on in vivo measurements on tobacco plants[84]. Γ*, C_a and O also vary with elevation, in direct proportion to atmospheric pressure.

The coordination hypothesis states that under typical daytime growth conditions photosynthesis is co-limited by carboxylation and electron transport. Optimal V_{cmax} is calculated as

$$V_{cmax,\,opt} = \varphi_0 I_{abs}[(C_i + K)/(C_i + 2\Gamma^*)] \quad (3)$$

where φ_0 is the intrinsic quantum efficiency of photosynthesis (mol C mol^{-1} photons); I_{abs} is the PPFD absorbed by the leaf (μmol photons m^{-2} s^{-1}). These values were corrected to 25°C using the Arrhenius equation with activation energies from Bernacchi et al.[84,85]. Intrinsic quantum efficiency was assumed to follow the temperature dependency of electron transport in light-adapted leaves[85]

$$\varphi_0 = (0.352 + 0.021\ T_g - 3.4 \times 10^{-4} T_g^2)/8 \quad (4)$$

According to Eq. (3) and its derivatives, optimal V_{cmax} increases in proportion to PPFD. It also increases with T_g. On the other hand, optimal V_{cmax25} *declines* with T_g. This is because the enzyme-kinetic effect, leading to a reduced V_{cmax25} requirement at higher temperatures (caused by the temperature dependency of Rubisco activity), is stronger than the photorespiratory effect, leading to an increased V_{cmax} requirement at higher temperatures (caused by the temperature dependencies of K and Γ*). Experimental manipulations of growth temperature[86], repeated measurements on the same plants at different seasons[24], global spatial patterns of V_{cmax}[11] and variations of V_{cmax25} on a long elevation transect[41] are all consistent with the negative temperature dependency of V_{cmax25} implied by Eq. (3).

Quantitative predictions of the effect of each climate variable on ln V_{cmax25} can be obtained by taking partial derivatives of Eq. (3) with respect to each variable in turn[21]. Logarithmic transformation is appropriate for magnitude variables described by multiplicative expressions like these[87]. The theory predicts approximately linear relationships of ln V_{cmax25} to ln PPFD, ln D and (without transformation) T_g[21]. These derivatives were evaluated at the median climate of the dataset (PPFD = 400 μmol m^{-2} s^{-1}, T_g = 25°C, D = 0.60 kPa) using the deriv package in R (ref. [88]) (Table 1).

Photosynthetic data. The leaf-trait dataset comprised measurements at 266 sites for a total of 1637 species and 5000 individuals, and soil measurements for 39% of sites (Fig. S2). The dataset consists of field measurements made in natural (unfertilized) vegetation, from several published data sources[7,8,14,20,28,73,89–94]. The numbers of species recorded within each PFT (ref. [95]) are provided in Table S3. V_{cmax} values were derived either from CO_2 response (A–C_i) curves (94% of the dataset) or the one-point method[6] from single measurements of light-saturated net photosynthesis (A_{sat}) (6% of the dataset). The one-point method provides a way to estimate V_{cmax} knowing only A_{sat}, day respiration (R_d), temperature and atmospheric pressure

$$V_{cmax}[\text{est}] \approx (A_{sat} + R_d)(C_i + K)/(C_i - \Gamma^*). \quad (5)$$

If no respiration measurement was available, the following approximation was used instead

$$V_{cmax}[\text{est}] \approx A_{sat}/[(C_i - \Gamma^*)/(C_i + K) - 0.015] \quad (6)$$

where R_d is assumed to be 1.5% of V_{cmax}[6,40,96]. Rogers et al.[97] indicated that the one-point method could result in a twofold underestimation of photosynthetic capacity in the Arctic region. Burnett et al.[98] however estimated errors in photosynthetic capacity at around 20% at most, suggesting that V_{cmax} data obtained in this way (which, in any case, constitute only a small fraction of the dataset) can be justified in the context of a global survey. If measurements were made at a temperature other than 25 °C, reported V_{cmax} and J_{max} values were standardized to 25° C using activation energies provided by Bernacchi et al.[84,85].

Climate data. Monthly average values of mean daily maximum (T_{max}, °C) and minimum (T_{min}, °C) temperatures were extracted at the 0.5° grid location of each site from Climate Research Unit data (CRU TS 4.01)[99], either for the measurement year or for the period 1991–2010 at sites not reporting measurement year. These data were three-dimensionally interpolated to actual site locations (longitude, latitude, elevation) using Geographically Weighted Regression (GWR) in ArcGIS. Mean daytime air temperature (T_g) was estimated for each month by assuming the diurnal temperature cycle to follow a sine curve, with daylight hours determined by latitude and month

$$T_g = T_{max}\left\{1/2 + (1 - x^2)^{1/2}/2\ \cos^{-1} x\right\} + T_{min}\left\{1/2 - (1 - x^2)^{1/2}/2\ \cos^{-1} x\right\},\ x = -\tan\lambda \tan\ \delta \quad (7)$$

where λ is latitude and δ is the monthly average solar declination[100]. Monthly values of T_g were averaged over the thermal growing season, i.e. months with mean daily temperature > 0 °C.

Incident solar radiation data were derived from WATCH Forcing Data ERA-Interim[101] at the same period and resolution, and also interpolated by GWR. Solar radiation (W m^{-2}) was converted to PPFD by multiplication by the energy-to-flux conversion factor 2.04 (μmol J^{-1})[102]. PPFD was averaged across the thermal growing season. Mean atmospheric pressures (P_{atm}) were derived using the barometric formula[102,103]. D (kPa) was estimated using the Magnus–Tetens

formula[46]

$$D = e_s - e_a, \quad (8)$$

with

$$e_s = 0.611\ \exp\left[17.27\ T/(T + 237.3)\right],\ \text{where}\ T = (T_{min} + T_{max})/2 \quad (9)$$

and

$$e_a = [P_{atm} W_{air} R_v]/[R_d + W_{air} R_v] \quad (10)$$

where W_{air} is the mass mixing ratio of water vapour to dry air; $W_{air} = q_{air}$ / (1 – q_{air}), where q_{air} is the specific humidity (kg/kg) derived from WATCH Forcing Data ERA-Interim[101], R_d and R_v are the specific gas constants of dry air and water vapour, $R_d = R/M_d$ and $R_v = R/M_v$, where R is the universal gas constant (8.314 J^{-1} K^{-1}), M_d is the molar mass of dry air (28.963 g mol^{-1}) and M_v is the molar mass of water vapour (18.02 g mol^{-1}).

Statistical analysis. The climate data were used to make theoretical predictions of relationships between photosynthetic capacity and climate variables based on the optimality framework, and independently, to derive statistical relationships by multiple regression (Tables S2 and S4). Separate statistical analyses were carried out for individual species, and for site-averaged measurements. In the analyses of individual species (i), each data-point represents the average of one or more measurements on a particular species at a site ($n = 2513$). In the analyses of site-averaged measurements (ii), each data-point represents an average for a site (across all individual and species; $n = 266$) (Table 1). Analyses of type (i) ('all species') data were carried out by means of a linear mixed effects model using the nlme package in R[88]. Climate variables (T_g, D, PPFD) were included as fixed terms, with site and species as random intercepts. A crossed rather than a fully nested random design was used because some species occurred at more than one site. Ordinary least squares multiple linear regression, using the lm function in R[88], was used for analyses of type (ii) ('site mean') data. Regression relationships were visualized using partial residual plots, obtained with the visreg package in R[88]. Partial residual plots display the relationship between values of the response variable versus each predictor variable, after those responses have been adjusted to hold all other predictors constant at their median values in the dataset. Photosynthetic capacities, PPFD and D were natural log-transformed before analysis so that the resulting regression coefficients can be directly compared with theoretical predictions (Table 1).

Model data comparisons. Model bias (B, %) in V_{cmax25} was calculated as follows:

$$B = 100\left(V_{cmax25}[\text{pred}] - V_{cmax25}[\text{obs}]\right)/V_{cmax25}[\text{obs}] \quad (11)$$

where V_{cmax25}[pred] is a predicted value and V_{cmax25}[obs] an observed value. Using theoretically predicted values, we explored whether B was significantly related to the climate variables. If so, this would indicate that the true responses of V_{cmax25} to climate variables were different from the predicted ones—pointing to something missing (or wrong) in the theory. Then, we explored whether bias in the values predicted by the statistical models (both all-species and site-mean models) was significantly related to leaf N_{area} and P_{area}. If found, such bias would indicate effects of leaf nutrients, additional to the effects of the climate variables considered.

Alternative models for the response to leaf nutrients. An alternative statistical model for photosynthetic capacity is a 'minimum function' of N_{area} or P_{area}[8]. The following differentiable equation is almost exactly equivalent to a minimum function (Fig. S3):

$$Z = -(1/k)\ \ln\left[e^{-kx} + e^{-ky}\right] \quad (12)$$

where Z is the response variable (V_{cmax25}), x and y are the predictor variables (N_{area}, P_{area}) and $k \gg 1$. Equation (12) is the 'log-sum-exp' formula, which provides a continuous approximation to the minimum function—allowing its use in regression, and comparison of goodness-of-fit statistics with ordinary linear regression (Table S2). The larger the value of k, the closer the approximation to the minimum function. A simple sensitivity analysis showed that large values of k (≥10) gave best performance (Table S5), indicating that the minimum function fitted the data better than a smooth transition between N and P limitation. Equation (12) was fitted to both all-species and site-mean data (Fig. 5). The equation was plotted using an iterative least squares procedure using the akima, stats and grDevices packages in R[88].

Statistics and reproducibility. Data collection, formulae and statistical analyses are described in 'Methods'. All statistical analyses used R software (ref. [88]), applying ordinary linear regression for site-mean analysis and a mixed effects model for all-species analysis. All R packages applied are referenced in 'Methods'. The relevant statistics for the main analyses are presented in Supplementary Information.

Reporting summary. Further information on research design is available in the Nature Research Reporting Summary linked to this article.

Data availability

No new data were collected for this analysis. The photosynthesis, leaf-trait and soils data are available from the authors of papers cited in the 'Methods' section[7,8,14,20,28,73,89–94]. The complete photosynthesis, climate, leaf-trait and soils datasets underlying all analyses are also publicly available at Zenodo[104] and GitHub: https://github.com/yunkepeng/VcmaxMS. In case of any issues concerning the observed and predicted data and for all queries on ancillary information including the climate data, please contact Y.P. (yunke.peng@usys.ethz.ch) or C.P. (c.prentice@imperial.ac.uk).

Received: 28 October 2020; Accepted: 10 March 2021;
Published online: 12 April 2021

References

1. De Kauwe, M. G. et al. Do land surface models need to include differential plant species responses to drought? Examining model predictions across a mesic-xeric gradient in Europe. *Biogeosciences* **12**, 7503–7518 (2015).
2. Smith, N. G. & Keenan, T. F. Mechanisms underlying leaf photosynthetic acclimation to warming and elevated CO2 as inferred from least-cost optimality theory. *Global Change Biol.* **26**, 5202–5216 (2020).
3. Farquhar, G. D., von Caemmerer, S. & Berry, J. A. A biochemical model of photosynthetic CO2 assimilation in leaves of C3 species. *Planta* **149**, 78–90 (1980).
4. Wullschleger, S. D. Biochemical limitations to carbon assimilation in C3 plants—a retrospective analysis of the A/Ci curves from 109 Species. *J. Exp. Bot.* **44**, 907–920 (1993).
5. Lloyd, J., Bloomfield, K., Domingues, T. F. & Farquhar, G. D. Photosynthetically relevant foliar traits correlating better on a mass vs an area basis: of ecophysiological relevance or just a case of mathematical imperatives and statistical quicksand? *New Phytol.* **199**, 311–321 (2013).
6. De Kauwe, M. G. et al. A test of the 'one-point method' for estimating maximum carboxylation capacity from field-measured, light-saturated photosynthesis. *New Phytol.* **210**, 1130–1144 (2015).
7. Ferreira Domingues, T. et al. Biome-specific effects of nitrogen and phosphorus on the photosynthetic characteristics of trees at a forest-savanna boundary in Cameroon. *Oecologia* **178**, 659–672 (2015).
8. Domingues, T. F. et al. Co-limitation of photosynthetic capacity by nitrogen and phosphorus in West Africa woodlands. *Plant, Cell Environ.* **33**, 959–980 (2010).
9. Walker, A. P. et al. The relationship of leaf photosynthetic traits -VcmaxandJmax- to leaf nitrogen, leaf phosphorus, and specific leaf area: a meta-analysis and modeling study. *Ecol. Evol.* **4**, 3218–3235 (2014).
10. Wang, H. et al. Towards a universal model for carbon dioxide uptake by plants. *Nat. Plants* **3**, 734–741 (2017).
11. Smith, N. G. et al. Global photosynthetic capacity is optimized to the environment. *Ecol. Lett.* **22**, 506–517 (2019).
12. Prentice, I. C., Dong, N., Gleason, S. M., Maire, V. & Wright, I. J. Balancing the costs of carbon gain and water transport: testing a new theoretical framework for plant functional ecology. *Ecol. Lett.* **17**, 82–91 (2014).
13. Givnish, T. J. *On the Economy of Plant Form and Function*: *Proceedings of the Sixth Maria Moors Cabot Symposium*, Vol. 6 (Cambridge University Press, 1986).
14. Maire, V. et al. Global effects of soil and climate on leaf photosynthetic traits and rates. *Glob. Ecol. Biogeogr.* **24**, 706–717 (2015).
15. Franklin, O. et al. Organizing principles for vegetation dynamics. *Nat. Plants* **6**, 444–453 (2020).
16. Ali, A. A. et al. A global scale mechanistic model of photosynthetic capacity (LUNA V1.0). *Geosci. Model Dev.* **9**, 587–606 (2016).
17. Dewar, R. et al. New insights into the covariation of stomatal, mesophyll and hydraulic conductances from optimization models incorporating nonstomatal limitations to photosynthesis. *New Phytol.* **217**, 571–585 (2017).
18. Caldararu, S., Thum, T., Yu, L. & Zaehle, S. Whole-plant optimality predicts changes in leaf nitrogen under variable CO 2 and nutrient availability. *New Phytol.* **225**, 2331–2346 (2019).
19. Wright, I. J. et al. The worldwide leaf economics spectrum. *Nature* **428**, 821–827 (2004).
20. Wang, H. et al. The China Plant Trait Database: toward a comprehensive regional compilation of functional traits for land plants. *Ecology* **99**, 500–500 (2017).
21. Wang, H. et al. Photosynthetic responses to altitude: an explanation based on optimality principles. *New Phytol.* **213**, 976–982 (2016).

22. Lavergne, A. et al. Historical changes in the stomatal limitation of photosynthesis: empirical support for an optimality principle. *New Phytol.* **225**, 2484–2497 (2019).
23. Maire, V. et al. The coordination of leaf photosynthesis links C and N fluxes in C3 plant species. *PLoS ONE* **7**, e38345 (2012).
24. Fürstenau Togashi, H. et al. Thermal acclimation of leaf photosynthetic traits in an evergreen woodland, consistent with the coordination hypothesis. *Biogeosciences* **15**, 3461–3474 (2018).
25. Kumarathunge, D. P. et al. Acclimation and adaptation components of the temperature dependence of plant photosynthesis at the global scale. *New Phytol.* **222**, 768–784 (2019).
26. Wright, I. J., Reich, P. B. & Westoby, M. Strategy shifts in leaf physiology, structure and nutrient content between species of high- and low-rainfall and high- and low-nutrient habitats. *Funct. Ecol.* **15**, 423–434 (2001).
27. Rogers, A. The use and misuse of V c,max in earth system models. *Photosynth. Res.* **119**, 15–29 (2013).
28. Dong, N. et al. Leaf nitrogen from first principles: field evidence for adaptive variation with climate. *Biogeosciences* **14**, 481–495 (2017).
29. Reich, P. B. & Schoettle, A. W. Role of phosphorus and nitrogen in photosynthetic and whole plant carbon gain and nutrient use efficiency in eastern white pine. *Oecologia* **77**, 25–33 (1988).
30. Raaimakers, D., Boot, R. G. A., Dijkstra, P. & Pot, S. Photosynthetic rates in relation to leaf phosphorus content in pioneer versus climax tropical rainforest trees. *Oecologia* **102**, 120–125 (1995).
31. Goll, D. S. et al. Nutrient limitation reduces land carbon uptake in simulations with a model of combined carbon, nitrogen and phosphorus cycling. *Biogeosciences* **9**, 3547–3569 (2012).
32. Reich, P. B., Oleksyn, J. & Wright, I. J. Leaf phosphorus influences the photosynthesis–nitrogen relation: a cross-biome analysis of 314 species. *Oecologia* **160**, 207–212 (2009).
33. Evans, J. R. Photosynthesis and nitrogen relationships in leaves of C3 plants. *Oecologia* **78**, 9–19 (1989).
34. Reich, P. B., Walters, M. B., Ellsworth, D. S. & Uhl, C. Photosynthesis-nitrogen relations in Amazonian tree species. *Oecologia* **97**, 62–72 (1994).
35. Kattge, J., Knorr, W., Raddatz, T. & Wirth, C. Quantifying photosynthetic capacity and its relationship to leaf nitrogen content for global-scale terrestrial biosphere models. *Global Change Biol.* **15**, 976–991 (2009).
36. Evans, J. R. & Clarke, V. C. The nitrogen cost of photosynthesis. *J. Exp. Bot.* **70**, 7–15 (2018).
37. Marschner, H. in *Mineral Nutrition of Higher Plants*, 405–435 (Elsevier, 1995).
38. Niinemets, Ü., Wright, I. J. & Evans, J. R. Leaf mesophyll diffusion conductance in 35 Australian sclerophylls covering a broad range of foliage structural and physiological variation. *J. Exp. Bot.* **60**, 2433–2449 (2009).
39. Malhi, Y. et al. The variation of productivity and its allocation along a tropical elevation gradient: a whole carbon budget perspective. *New Phytol.* **214**, 1019–1032 (2016).
40. Wang, H. et al. Acclimation of leaf respiration consistent with optimal photosynthetic capacity. *Global Change Biol.* **26**, 2573–2583 (2020).
41. Peng, Y., Bloomfield, K. J. & Prentice, I. C. A theory of plant function helps to explain leaf-trait and productivity responses to elevation. *New Phytol.* **226**, 1274–1284, (2020).
42. Gvozdevaite, A. et al. Leaf-level photosynthetic capacity dynamics in relation to soil and foliar nutrients along forest–savanna boundaries in Ghana and Brazil. *Tree Physiol.* **38**, 1912–1925 (2018).
43. Terrer, C. et al. Nitrogen and phosphorus constrain the CO 2 fertilization of global plant biomass. *Nat. Clim. Change* **9**, 684–689 (2019).
44. Meir, P. et al. in *Advances in Photosynthesis and Respiration*, 89–105 (Springer International Publishing, 2017).
45. Luo, X. & Keenan, T. F. Global evidence for the acclimation of ecosystem photosynthesis to light. *Nat. Ecol. Evol.* **4**, 1351–1357 (2020).
46. Stocker, B. D. et al. P-model v1.0: an optimality-based light use efficiency model for simulating ecosystem gross primary production. *Geosci. Model Dev.* **13**, 1545–1581 (2020).
47. Lavergne, A., Sandoval, D., Hare, V. J., Graven, H. & Prentice, I. C. Impacts of soil water stress on the acclimated stomatal limitation of photosynthesis: insights from stable carbon isotope data. *Global Change Biol.* **26**, 7158–7172 (2020).
48. Zhou, S., Duursma, R. A., Medlyn, B. E., Kelly, J. W. G. & Prentice, I. C. How should we model plant responses to drought? An analysis of stomatal and non-stomatal responses to water stress. *Agric. For. Meteorol.* **182-183**, 204–214 (2013).
49. Zhou, S. et al. Short-term water stress impacts on stomatal, mesophyll and biochemical limitations to photosynthesis differ consistently among tree species from contrasting climates. *Tree Physiol.* **34**, 1035–1046 (2014).
50. Katul, G., Manzoni, S., Palmroth, S. & Oren, R. A stomatal optimization theory to describe the effects of atmospheric CO2 on leaf photosynthesis and transpiration. *Ann. Bot.* **105**, 431–442 (2009).
51. Manzoni, S. et al. Optimizing stomatal conductance for maximum carbon gain under water stress: a meta-analysis across plant functional types and climates. *Funct. Ecol.* **25**, 456–467 (2011).
52. Medlyn, B. E. et al. Reconciling the optimal and empirical approaches to modelling stomatal conductance. *Global Change Biol.* **17**, 2134–2144 (2011).
53. Crous, K. Y. et al. Photosynthesis of temperate *Eucalyptus globulus* trees outside their native range has limited adjustment to elevated CO2 and climate warming. *Global Change Biol.* **19**, 3790–3807 (2013).
54. Zhou, S.-X., Medlyn, B. E. & Prentice, I. C. Long-term water stress leads to acclimation of drought sensitivity of photosynthetic capacity in xeric but not riparian *Eucalyptus* species. *Ann. Bot.* **117**, 133–144 (2015).
55. Smith, N. G. & Dukes, J. S. Short-term acclimation to warmer temperatures accelerates leaf carbon exchange processes across plant types. *Global Change Biol.* **23**, 4840–4853 (2017).
56. Katul, G., Leuning, R. & Oren, R. Relationship between plant hydraulic and biochemical properties derived from a steady-state coupled water and carbon transport model. *Plant, Cell Environ.* **26**, 339–350 (2003).
57. Stocker, B. D. et al. Quantifying soil moisture impacts on light use efficiency across biomes. *New Phytol.* **218**, 1430–1449 (2018).
58. Kattge, J. & Knorr, W. Temperature acclimation in a biochemical model of photosynthesis: a reanalysis of data from 36 species. *Plant, Cell Environ.* **30**, 1176–1190 (2007).
59. van der Plas, F. et al. Plant traits alone are poor predictors of ecosystem properties and long-term ecosystem functioning. *Nat. Ecol. Evol.* **4**, 1602–1611 (2020).
60. Quesada, M. et al. Succession and management of tropical dry forests in the Americas: review and new perspectives. *For. Ecol. Manag.* **258**, 1014–1024 (2009).
61. Phillips, O. L. et al. Drought–mortality relationships for tropical forests. *New Phytol.* **187**, 631–646 (2010).
62. Laliberté, E., Lambers, H., Burgess, T. I. & Wright, S. J. Phosphorus limitation, soil-borne pathogens and the coexistence of plant species in hyperdiverse forests and shrublands. *New Phytol.* **206**, 507–521 (2014).
63. Conroy, J. P., Smillie, R. M., Küppers, M., Bevege, D. I. & Barlow, E. W. Chlorophyll a fluorescence and photosynthetic and growth responses of pinus radiata to phosphorus deficiency, drought stress, and high CO2. *Plant Physiol.* **81**, 423–429 (1986).
64. Loustau, D., Brahim, M. B., Gaudillere, J. P. & Dreyer, E. Photosynthetic responses to phosphorus nutrition in two-year-old maritime pine seedlings. *Tree Physiol.* **19**, 707–715 (1999).
65. Warren, C. R. & Adams, M. A. Phosphorus affects growth and partitioning of nitrogen to Rubisco in *Pinus pinaster*. *Tree Physiol.* **22**, 11–19 (2002).
66. Bloomfield, K. J., Farquhar, G. D. & Lloyd, J. Photosynthesis–nitrogen relationships in tropical forest tree species as affected by soil phosphorus availability: a controlled environment study. *Funct. Plant Biol.* **41**, 820–832 (2014).
67. Crous, K. Y., Ósvaldsson, A. & Ellsworth, D. S. Is phosphorus limiting in a mature *Eucalyptus* woodland? Phosphorus fertilisation stimulates stem growth. *Plant Soil* **391**, 293–305 (2015).
68. Sivak, M. N. & Walker, D. A. Photosynthesis in vivo can be limited by phosphate supplY. *New Phytol.* **102**, 499–512 (1986).
69. Kiirats, O., Cruz, J. A., Edwards, G. E. & Kramer, D. M. Feedback limitation of photosynthesis at high CO2 acts by modulating the activity of the chloroplast ATP synthase. *Funct. Plant Biol.* **36**, 893–901 (2009).
70. Ellsworth, D. S., Crous, K. Y., Lambers, H. & Cooke, J. Phosphorus recycling in photorespiration maintains high photosynthetic capacity in woody species. *Plant, Cell Environ.* **38**, 1142–1156 (2015).
71. Zhang, S. & Dang, Q. L. Effects of carbon dioxide concentration and nutrition on photosynthetic functions of white birch seedlings. *Tree Physiol.* **26**, 1457–1467 (2006).
72. Lambers, H. et al. Proteaceae from severely phosphorus-impoverished soils extensively replace phospholipids with galactolipids and sulfolipids during leaf development to achieve a high photosynthetic phosphorus-use-efficiency. *New Phytol.* **196**, 1098–1108 (2012).
73. Meir, P., Levy, P. E., Grace, J. & Jarvis, P. G. Photosynthetic parameters from two contrasting woody vegetation types in West Africa. *Plant Ecol.* **192**, 277–287 (2007).
74. Kull, O. Acclimation of photosynthesis in canopies: models and limitations. *Oecologia* **133**, 267–279 (2002).
75. Field, C. & Mooney, H. in *On the Economy of Plant Form and Function*: *Proceedings of the Sixth Maria Moors Cabot Symposium*, *Evolutionary Constraints on Primary Productivity, Adaptive Patterns of Energy Capture in Plants, Harvard Forest*, *August 1983* (Cambridge University Press, 1986).
76. Niinemets, Ü. Research review. Components of leaf dry mass per area - thickness and density - alter leaf photosynthetic capacity in reverse directions in woody plants. *New Phytol.* **144**, 35–47 (1999).

77. Lloyd, J. et al. Optimisation of photosynthetic carbon gain and within-canopy gradients of associated foliar traits for Amazon forest trees. *Biogeosciences* **7**, 1833–1859 (2010).
78. Anten, N. P. R. Optimal photosynthetic characteristics of individual plants in vegetation stands and implications for species coexistence. *Ann. Bot.* **95**, 495–506 (2004).
79. Alton, P. B. & North, P. Interpreting shallow, vertical nitrogen profiles in tree crowns: a three-dimensional, radiative-transfer simulation accounting for diffuse sunlight. *Agric. For. Meteorol.* **145**, 110–124 (2007).
80. Rogers, A. et al. A roadmap for improving the representation of photosynthesis in Earth system models. *New Phytol.* **213**, 22–42 (2017).
81. Tosens, T. & Laanisto, L. Mesophyll conductance and accurate photosynthetic carbon gain calculations. *J. Exp. Bot.* **69**, 5315–5318 (2018).
82. Niinemets, Ü., Díaz-Espejo, A., Flexas, J., Galmés, J. & Warren, C. R. Importance of mesophyll diffusion conductance in estimation of plant photosynthesis in the field. *J. Exp. Bot.* **60**, 2271–2282 (2009).
83. Farquhar, G. D., O'Leary, M. H. & Berry, J. A. On the relationship between carbon isotope discrimination and the intercellular carbon dioxide concentration in leaves. *Funct. Plant Biol.* **9**, 121–137 (1982).
84. Bernacchi, C. J., Singsaas, E. L., Pimentel, C., Portis, A. R. Jr & Long, S. P. Improved temperature response functions for models of Rubisco-limited photosynthesis. *Plant, Cell Environ.* **24**, 253–259 (2001).
85. Bernacchi, C. J., Pimentel, C. & Long, S. P. In vivo temperature response functions of parameters required to model RuBP-limited photosynthesis. *Plant, Cell Environ.* **26**, 1419–1430 (2003).
86. Scafaro, A. P. et al. Strong thermal acclimation of photosynthesis in tropical and temperate wet-forest tree species: the importance of altered Rubisco content. *Global Change Biol.* **23**, 2783–2800 (2017).
87. Warton, D. I., Wright, I. J., Falster, D. S. & Westoby, M. Bivariate line-fitting methods for allometry. *Biol. Rev.* **81**, 259–291 (2006).
88. Team, R. C. *R.: a Language and Environment for Statistical Computing* (R Foundation for Statistical Computing, 2018).
89. Atkin, O. K. et al. Global variability in leaf respiration in relation to climate, plant functional types and leaf traits. *New Phytol.* **206**, 614–636 (2015).
90. Bahar, N. H. A. et al. Leaf-level photosynthetic capacity in lowland Amazonian and high-elevation Andean tropical moist forests of Peru. *New Phytol.* **214**, 1002–1018 (2016).
91. Bloomfield, K. J. et al. The validity of optimal leaf traits modelled on environmental conditions. *New Phytol.* **221**, 1409–1423 (2018).
92. Cernusak, L. A., Hutley, L. B., Beringer, J., Holtum, J. A. M. & Turner, B. L. Photosynthetic physiology of eucalypts along a sub-continental rainfall gradient in northern Australia. *Agric. For. Meteorol.* **151**, 1462–1470 (2011).
93. Xu, H. Y., et al. Predictability of leaf traits with climate and elevation: a case study in Gongga Mountain, China. *Tree Physiol.* https://doi.org/10.1093/treephys/tpab003 (2021).
94. Walker, A. P., et al. *A Global Data Set of Leaf Photosynthetic Rates, Leaf N and P, and Specific Leaf Area* (Oak Ridge National Laboratory Distributed Active Archive Center, 2014). https://doi.org/10.3334/ORNLDAAC/1224.
95. Kattge, J. et al. TRY–a global database of plant traits. *Global Change Biol.* **17**, 2905–2935 (2011).
96. Collatz, G. J., Ribas-Carbo, M. & Berry, J. A. Coupled photosynthesis-stomatal conductance model for leaves of C4 plants. *Funct. Plant Biol.* **19**, 519 (1992).
97. Rogers, A., Serbin, S. P., Ely, K. S., Sloan, V. L. & Wullschleger, S. D. Terrestrial biosphere models underestimate photosynthetic capacity and CO2 assimilation in the Arctic. *New Phytol.* **216**, 1090–1103 (2017).
98. Burnett, A. C., Davidson, K. J., Serbin, S. P. & Rogers, A. The "one-point method" for estimating maximum carboxylation capacity of photosynthesis: a cautionary tale. *Plant, Cell Environ.* **42**, 2472–2481 (2019).
99. Harris, I., Jones, P. D., Osborn, T. J. & Lister, D. H. Updated high-resolution grids of monthly climatic observations–the CRU TS3.10 Dataset. *Int. J. Climatol.* **34**, 623–642 (2013).
100. Jones, H. G. *Plants and Microclimate* (Cambridge University Press, 2009).
101. Weedon, G. P. et al. The WFDEI meteorological forcing data set: WATCH forcing data methodology applied to ERA-interim reanalysis data. *Water Resour. Res.* **50**, 7505–7514 (2014).
102. Davis, T. W. et al. Simple process-led algorithms for simulating habitats (SPLASH v.1.0): robust indices of radiation, evapotranspiration and plant-available moisture. *Geosci. Model Dev.* **10**, 689–708 (2017).
103. Berberan-Santos, M. N., Bodunov, E. N. & Pogliani, L. On the barometric formula. *Am. J. Phys.* **65**, 404–412 (1997).
104. Peng, Y., et al. *Dataset of Global Climate and Nutrient Controls of Photosynthetic Capacity* (Zenodo, 2021). https://doi.org/10.5281/zenodo.4568148.

Acknowledgements

The authors thank Professor Jon Lloyd for help with obtaining data and many scientific discussions. The authors also thank Tiina Tosens for a helpful review of an earlier draft. This research has received funding from the European Research Council (ERC) under the European Union's Horizon 2020 research and innovation programme (grant agreement no: 787203 REALM) and it is a contribution to the Imperial College initiative on Grand Challenges in Ecosystems and the Environment. The authors thank Owen Atkin, Vincent Maire, Anthony Walker, Han Wang and Huiying Xu for contributing published and/or unpublished data for these analyses. Yanzheng Yang and Yuhui Wu assisted with data collection in China, during fieldwork supported by the National Natural Science Foundation of China (grant agreement nos: 91837312, 31971495). Some data used were collected as part of the UK Natural Environment Research Council consortium 'Tropical Biomes In Transition' (TROBIT) (grant agreement no: NE/D01185x/1) to the University of Edinburgh. Further data were collected within the Nordeste project, supported in Brazil by FAPESP (grant agreement no: 2015-50488-5) and in the UK by NERC and the Newton Fund (grant agreement no: NE/N01256/1).

Author contributions

I.C.P. proposed the topic and supervised the research. Y.P. carried out all analyses, created the graphics and wrote the first draft of the manuscript. All authors provided data for the analysis and contributed to the interpretation of results and revisions of the manuscript.

Competing interests

The authors declare no competing interests.

Additional information

Supplementary information The online version contains supplementary material available at https://doi.org/10.1038/s42003-021-01985-7.

Correspondence and requests for materials should be addressed to I.C.P.

Reprints and permission information is available at http://www.nature.com/reprints.

Publisher's note Springer Nature remains neutral with regard to jurisdictional claims in published maps and institutional affiliations.